Research On Interior Permanent Magnet Synchronous Motor Based on Performance Matching of Electric Bus

Yongming Xu, Mengmeng Ai, Ziyi Xu, Wenhui Liu, and Yaodong Wang

***Abstract*—The interior permanent magnet (IPM) motor is commonly used as the drive motor for the electric car due to high torque density, high efficiency, and good field weakening speed regulation capabilities. In this paper, an 80kW IPM motor with uneven air gap is designed as a drive motor for an electric bus. The total weight of the electric bus is 11000 kg, and its length/width/height is 8190/2400/2960 mm, respectively. In-depth analysis and research have also been conducted on the power parameter coordination between the IPM motor and the electric bus. The operational and mechanical characteristic curves of the drive motor under a straight-line driving cycle are analyzed through simulation, and the simulation results are verified through experiments. Comparing the results of simulation and experiment, it is known that the error of the rated torque is as high as 4.8%, and the error of the peak torque is as high as 8.6%.**

***Index Terms*—Driving cycle, electric machine design, IPM, motor torque, power parameter coordination.**

I. Introduction

In order to reduce greenhouse gas emissions and save non-renewable energy, the world is accelerating the process of electrification of vehicles. Permanent magnet synchronous motors (PMSM) are commonly used as electric vehicle traction motors due to high power/torque density, high efficiency and good field weakening ability [1]–[3]. The interior permanent magnet (IPM) motor has a larger saliency, excellent overload capacity and stability, and wider speed range operation [4], [5]. Therefore, the IPM motor has become a commonly used driving motor for electric vehicles, such as Tesla Model 3, BMW i3, Porsche Taycan, etc.

When designing the drive motor, the power parameter coordination is an important factor to judge whether the design is reasonable. A few studies have been undertaken to provide a fundamental understanding of this [6], [7]. For the IPM motor, researchers have done a lot of researches on the permanent magnet structure, uneven air gap, torque ripple, cogging torque suppression, winding mode, and overload capacity [8]–[10]. The above researches primarily concentrate on the design or performance analysis of motor body of the IPM motor. Too little work has been devoted to the dynamic characteristics of the IPM motor and its influencing factors on electric vehicles. Therefore, further researches in this field are necessary. This study aims to contribute to this growing area of researches by exploring the dynamic characteristics of an 80 kW IPM motor and the impact of uneven air gap on performance through simulation analysis and experimental verification.

Manuscript received February 26, 2021; revised April 15, 2021; accepted May 14, 2021. Date of publication June 21, 2021; date of current version July 30, 2021. This work was supported in part by the National Science Foundation of China under Grant 52077047 and in part by Natural Science Foundation of Heilongjiang Province, China, under Grant LH2020E092. *(Corresponding author:Yongming Xu.)*

Yongming Xu, Mengmeng Ai, and Ziyi Xu are with the School of Electrical and Electronic Engineering, Harbin University of Science and Technology, Harbin 150080, China (e-mail: xuyongming@hrbust.edu.cn).

Wenhui Liu is with the Harbin Electric Corporation Jiamusi Electric Machine Company, Ltd., Jiamusi 154000, China (e-mail: jmsliuwenhui@163.com).

Yaodong Wang is with the Durham University, Durham DH1 3LE, U.K. (e-mail: yaodong.wang@durham.ac.uk).

Color versions of one or more figures in this article are available at https://doi.org/10.1109/TASC.2021.3091062.

Digital Object Identifier 10.1109/TASC.2021.3091062

II. Dynamic Calculation of the Pure Electric Bus

A. Parameters of Pure Electric Bus

Considering that buses travel on smooth urban roads and their speed is limited, the performance requirements of the bus are shown in Table I.

B. Power Parameter Matching

When designing the drive motor, it is necessary to ensure that the power parameters of the IPM motor and the bus match reasonably so that the dynamic characteristics of the IPM motor can meet the power requirements of the bus under different driving cycle [11]. The power of the IPM motor is crucial to the dynamic performance of the electric vehicle. During the driving process of the car, the drive motor's output power is balanced with the resistance power of the driving. Therefore, at every moment, the drive motor's power is equal to the mechanical transmission's power and the power of all resistance to motion [12]. The performance index requirements of the drive motor are shown in Table II.

III. Simulation

Use simulation analysis software Ansoft Maxwell to perform 2D finite element analysis on the IPM motor. Considering the symmetry of the internal structure of the IPM motor, a 1/8 simulation analysis model is established to analyze the transient magnetic field of the IPM motor, as shown in Fig. 1. Moreover, the detailed parameters of the IPM motor are summarized in Table III.

The performance of the permanent magnet plays an important role in the performance of the permanent magnet motor. The permanent magnet material selected for this motor is N38UH,

TABLE I
BUS PERFORMANCE

Symbol	Items	Value
$l/w/h$	Length/Width/Height (mm)	8190*2400*2960
A	Frontal area (m^2)	6.1
m_0	Vehicle mass (kg)	7950
m	Maximum total mass (kg)	11000
r	Wheel rolling radius (m)	0.453
C_D	Air resistance coefficient	0.61
f	Rolling resistance coefficient	0.012
η_t	Transmission efficiency	0.93
i_0	Gear transmission ratio	4.93
i_g	Transmission ratio of transmission	1.41
v_{max}	Speed (km/h)	<70
a	Maximum climbing rate under full load	$\geq$20%
v_i	Maximum climbing speed at full load (km/h)	$\geq$15
t_a	Acceleration time (s)	$\leq$25(0-50km/h)

TABLE II
PERFORMANCE REQUIREMENTS OF DRIVE MOTOR

Symbol	Items	Value
P_{max}	Maximum power (kW)	$\geq$126
n_{max}	Maximum speed (rpm)	$\geq$2849
T_{max}	Maximum torque (N·m)	$\geq$1573
η	Maximum efficiency in electric state	$\geq$95%
	Ratio of efficient work area ($\geq$ 80%) to total work area	$\geq$90%

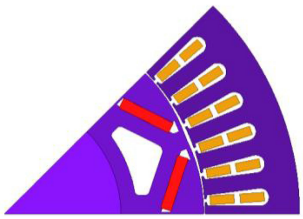

Fig. 1. The 1/8-part 2D model of the IPM motor.

TABLE III
DETAILED PARAMETER OF THE IPM MOTOR

Symbol	Items	Value
P_N	Rated power (kW)	80
P_{max}	Maximum power (kW)	130
U_N	Rated phase voltage (V)	220
f_n	Frequency (Hz)	83.33
n_N	Rated speed (rpm)	1250
T_N	Rated torque (N·m)	611
T_{max}	Maximum torque (N·m)	1700
	Phase number	3
P	Polar number	4
Q	Slot number	48
D_1	Stator outer diameter (mm)	380
D_{i1}	Stator inner diameter (mm)	258.4
L_a	Iron core length (mm)	200
D_{r1}	Maximum rotor outer diameter (mm)	256.7
D_{r2}	Minimum rotor outer diameter (mm)	253.3
T_{ep}	Maximum Working temperature (°C)	180
	Material of permanent magnet	N38UH

which its Br and Hc are 1.06 T and 782.65 kA/m at 180 °C. By simulation, the magnetic induction intensity B = 0.67 T, while the knee point K is 0.4 T at 180 °C for N38UH, so permanent magnet will not lose its magnetism permanently when it works at 180 °C.

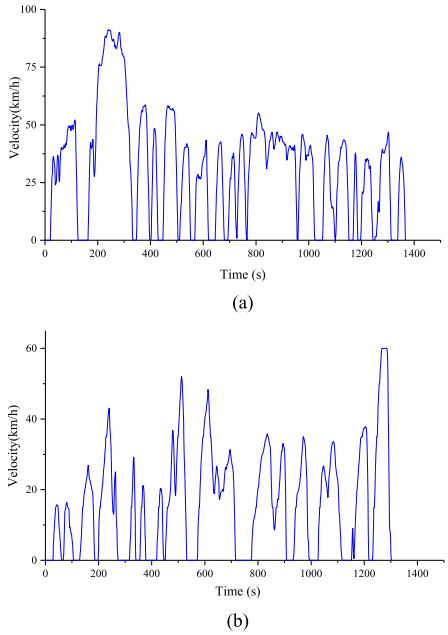

Fig. 2. Driving cycle velocity profiles. (a) UDDS. (b) Typical Bus Driving Cycle in China.

IV. ELECTRIC BUS DRIVING CYCLE

In order to verify the power parameter matching between the drive motor and the electric bus, the driving cycles of the motor and the bus are simulated by using the Motor-CAD simulation software. The driving cycle is designed to simulate repeatable urban driving conditions. Its main function is to measure the consumption and emissions of cars. The principle of driving cycle is a "scenario" that simulates the acceleration/deceleration and speed of a car in a given time [13], [14].

A. Specification of the Investigated Driving Cycles

This article considers two typical driving cycles. The first is the urban dynamometer driving schedule (UDDS), which is suitable for urban driving, as shown in Fig. 2(a). It represents a city driving condition with frequent start and stop, and drive motors mostly run in low-speed areas. The second, Typical Bus Driving Cycle in China, which is based on driving conditions of urban buses in China. The maximum speed is 60 km/h, and the average speed is 16.11 km/h, as shown in Fig. 2(b).

For UDDS, the simulation result of the drive motor is shown in Fig. 3(a), and the maximum torque is 1239.5 N·m in this cycle.

For Typical Bus Driving Cycle in China, the simulation result of the drive motor is shown in Fig. 3(b), and the maximum torque is 1065 N·m in this cycle.

B. Climbing Ability

As a bus with a weight of 11000 kg, it needs to meet the gradient requirement when driving in the city. Table IV shows the output performance of motors for buses at different speed and gradient. The bus can pass through 20 % gradient at 15 km/h and 10% gradient at 30 km/h, which meets the performance requirements on uphill.

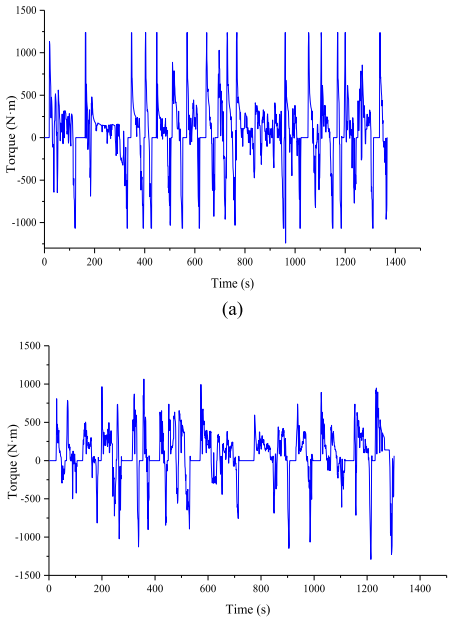

Fig. 3. Driving cycle torque profiles. (a) UDDS. (b) Typical Bus Driving Cycle in China.

TABLE IV
CLIMBING ABILITY

Gra-dient	15km/h			30km/h		
	T (N·m)	P (kW)	η	T (N·m)	P (kW)	η
5%	470.5	30.1	93.1%	478.6	61.2	94.1%
10%	844.6	54	92.5%	852.9	109.1	94.6%
15%	1213	77 .6	90.6%			
20%	1573	126	87.1%			

Fig. 4. The experimental platform.

V. EXPERIMENTAL VALIDATIONS

According to the results of simulation and power performance parameters matching, an IPM motor sample was manufactured. In order to validate the correctness of theory and numerical simulation results, a prototype testing platform has been built, as shown in Fig. 4. The torque-speed characteristics of the motor can be obtained through experiments. The torque-speed characteristic characterizes the output capacity and dynamic characteristic of the motor. Whether the designed motor meets the requirements of electric passenger cars can be judged according to the torque-speed characteristic curve.

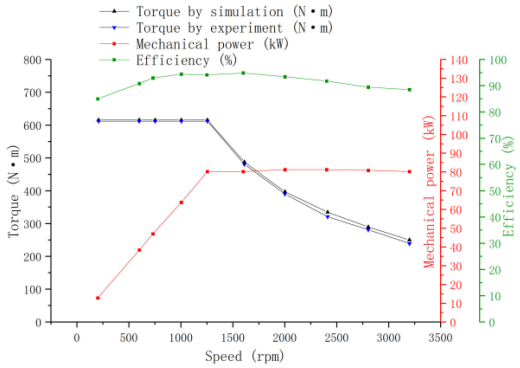

Fig. 5. Motor dynamic characteristic curve under rated state.

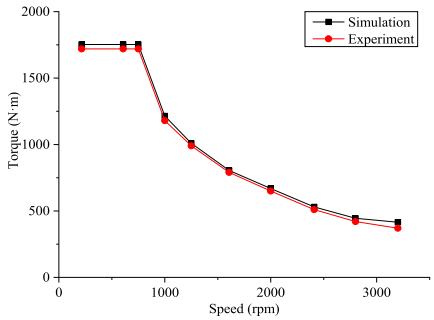

Fig. 6. Maximum torque-speed characteristic curves of the prototype.

A. Rated State

Fig. 5 shows the experimental and simulation results of the dynamic characteristic curve under rated operating conditions. In this figure, two black lines are the torque-speed characteristic curve obtained from the experiment and simulation, respectively. It can be known that the torque of the IPM motor under the constant torque condition is 611 N·m, and the error of the experiment and simulation in the entire constant torque range is less than 1%. When the motor speed rises to 3200 rpm under constant power conditions, the error between experiment and simulation is the largest, up to 4.8%. The green line represents the motor efficiency-speed curve, and the red line represents the mechanical power output by the motor. It can be seen from the curve that the efficiency of the motor has been maintained at a very high level under the rated state and the motor outputs mechanical power stably in the entire speed range. This proves the rationality of the designed motor. Fig. 5 shows that when the motor is running under rated conditions, the dynamic characteristic curve obtained by the simulation is consistent with the curve obtained by the experiment. This proves the accuracy of the numerical simulation results.

B. Peak State

Fig. 6 shows the dynamic characteristic curves of the motor through experiment and simulation under peak conditions. Analyzing Fig. 6 shows that the peak torque of the motor is 1711 N·m. The maximum torque of the motor is larger than the required torque under different driving cycles and slopes calculated in the fourth section, which proves that the designed motor meets the

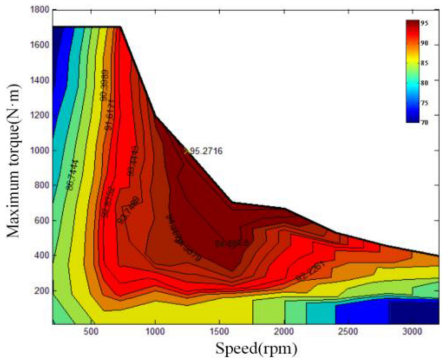

Fig. 7. Measured efficiency map of the designed IPM motor.

requirements. And when the motor runs under peak conditions, its speed is less than 750 rpm. When the motor output torque is the peak torque, the maximum error of the two curves in the Fig. 6 is 2.8%. The torque is decreased with the increase of speed; the minimum torque is 370 N·m at the speed of 3200 rpm, and the error between simulation and experiment is 8.6%. The analysis result show that the experimental and simulation results of the dynamic characteristics of the IPM motor are consistent under peak conditions.

C. Efficiency Map of the PMSM

The efficiency map of the IPM motor within the maximum allowable torque and speed range is shown in Fig. 7. The high-efficiency operation area (efficiency $\geq$80%) of the drive motor occupies for 90.5% of the total operation area, and the maximum efficiency is 95.6%. It can be seen that the IPM motor designed in this paper basically meets the power and operating requirements of electric buses.

VI. Conclusion

In this work, an IPM motor with high material utilization and high efficiency was designed and manufactured. Based on the dynamic characteristic calculation method, the power parameters of the drive motor and the bus were matched. Firstly, the parameters of the electric bus were collected, and then the road traffic information of the electric bus was collected. The required torque of the motor can be calculated according to the curve of the speed-time under different driving cycles. According to the calculated torque-time curve, the torque requirement of the motor can be determined. After that, the output torque of the motor is calculated by simulation. Finally, the experiment verified dynamic characteristics of the motor. The experimental results proved the accuracy of the simulation analysis, and the designed motor meets the requirements of the electric bus. The designed IPM can realize the stable operation in UDDS and Typical Bus Driving Cycle in China.

References

[1] S. Fang, H. Liu, H. Wang, H. Yang, and H. Lin, "High power density PMSM with lightweight structure and high-performance soft magnetic alloy core," *IEEE Trans. Appl. Supercond.*, vol. 29, no. 2, Mar. 2019, Art. no. 0602805.

[2] Y. Zhang, W. Cao, S. McLoone, and J. Morrow, "Design and flux-weakening control of an interior permanent magnet synchronous motor for electric vehicles," *IEEE Trans. Appl. Supercond.*, vol. 26, no. 7, Oct. 2016, Art. no. 0606906.

[3] M. Popescu, J. Goss, D. A. Staton, D. Hawkins, Y. C. Chong, and A. Boglietti, "Electrical vehicles—Practical solutions for power traction motor systems," *IEEE Trans. Ind. Appl.*, vol. 54, no. 3, pp. 2751–2762, May/Jun. 2018.

[4] G. Pellegrino, A. Vagati, P. Guglielmi, and B. Boazzo, "Performance comparison between surface-mounted and interior PM motor drives for electric vehicle application," *IEEE Trans. Ind. Electron.*, vol. 59, no. 2, pp. 803–811., Feb. 2012.

[5] Z. Nan and N. Schofield, "Field-weakening capability of interior permanent-magnet machines with salient pole shoe rotors," *IEEE Trans. Magn.*, vol. 53, no. 11, Nov. 2017, Art. no. 8112607.

[6] A. G. Sarigiannidis, M. E. Beniakar, and A. G. Kladas, "Fast adaptive evolutionary PM traction motor optimization based on electric vehicle drive cycle," *IEEE Trans. Veh. Technol.*, vol. 66, no. 7, pp. 5762–5774, Jul. 2017.

[7] O. Farrok, M. R. Islam, Y. Guo, J. Zhu, and W. Xu, "A novel design procedure for designing linear generators," *IEEE Trans. Ind. Electron.*, vol. 65, no. 2, pp. 1846–1854, Feb. 2018.

[8] J. Rao, Y. Gao, D. Li, and R. Qu, "Performance analysis of interior permanent magnet motor using overlapping windings with fractional ratio of slot to pole pair," *IEEE Trans. Appl. Supercond.*, vol. 26, no. 7, Oct. 2016, Art. no. 0610005.

[9] H. Jang, S. Oh, Y. Park, H. Kim, I. S. Jang, and J. Lee, "Design and analysis of a novel rotor shape to improve power performance," *IEEE Trans. Appl. Supercond.*, vol. 30, no. 4, Jun. 2020, Art. no. 5201304.

[10] J. Du, X. Wang, and H. Lv, "Optimization of magnet shape based on efficiency map of IPMSM for EVs," *IEEE Trans. Appl. Supercond.*, vol. 26, no. 7, Oct. 2016, Art. no. 0609807.

[11] G. Du, W. Cao, S. Hu, Z. Lin, and T. Yuan, "Design and assessment of an electric vehicle powertrain model based on real-world driving and charging cycles," *IEEE Trans. Veh. Technol.*, vol. 68, no. 2, pp. 1178–1187, Feb. 2019.

[12] X. Sun, Z. Shi, G. Lei, Y. Guo, and J. Zhu, "Analysis and design optimization of a permanent magnet synchronous motor for a campus patrol electric vehicle," *IEEE Trans. Veh. Technol*, vol. 68, no. 11, pp. 10,535–10,544, Nov. 2019.

[13] C. T. Krasopoulos, M. E. Beniakar, and A. G. Kladas, "Multicriteria PM motor design based on ANFIS evaluation of EV driving cycle efficiency," *IEEE Trans. Transp. Electrif.*, vol. 4, no. 2, pp. 525–535, Jun. 2018.

[14] H. Chen, X. Liu, N. A. O. Demerdash, A. M. EL-Refaie, Z. Chen, and J. He, "Computationally efficient optimization of a five-phase flux-switching PM machine under different operating conditions," *IEEE Trans. Veh. Technol.*, vol. 68, no. 7, pp. 6495–6508, Jul. 2019.